

Multimodal Approach for Kayaking Performance Analysis and Improvement

Nagy, G.^{1,2}, Komka, Zs.^{1,3,7}, Szathmáry, G.¹, Katona, P.^{1,4}, Gannoruwa, L.⁴,

Erdős, G.⁵, Tarjányi, P.⁹, Tóth, M.⁷, Krepuska, M.^{1,6}, Grand, L.^{1,5,8}

¹ Faculty of Information Technology and Bionics, Pázmány Péter Catholic University, Hungary

² Department of Telecommunications and Media Informatics, Budapest University of Technology and Economics, Hungary

³ Heart and Vascular Center, Semmelweis University, Hungary

⁴ Department of Kinesiology, University of Physical Education, Hungary

⁵ Institute of Advanced Studies, Hungary

⁶ Department of Medical Imaging, Semmelweis University, Hungary

⁷ Department of Health Sciences and Sport Medicine, University of Physical Education, Hungary

⁸ Neurology and Neurosurgery, The Johns Hopkins Hospital, United States

⁹ Polaritás-GM Ltd, Budapest, Hungary

Abstract

Artificial Intelligence (AI) invades fields where sophisticated analytics has not been applied before. Modality refers to how something happens or is experienced. Multimodal datasets are beneficial for solving complex research problems with AI methods. Kayaking technique optimization has been challenging, as there seems to be no gold standard for effective paddling techniques since there are outstanding athletes with profoundly different physical capabilities and kayaking styles.

Multimodal analysis can help find the most effective paddling techniques for training and competition based on individuals' abilities.

We describe the characteristics of the output power of kayak athletes and Electromyogram (EMG) measurements collected from the most critical muscles, and the relationship between these modalities. We propose metrics (weighted arithmetic mean difference and variability of power output and stroke duration) suitable for discerning athletes based on how efficiently and correctly they perform particular training tasks. Additionally, the described methods (asymmetry, coactivation, muscle intensity-output power) help athletes and coaches in assessing their performance and compare it with others based on their EMG activities.

As the next step, we will apply machine-learning approaches on the synchronized dataset we collect with the described methods to reveal desirable EMG and stroke patterns.

KEYWORDS: KAYAKING TECHNIQUE ANALYSIS, KAYAKING PERFORMANCE, SPORTS ANALYTICS, MAXIMAL INTENSITY EXERCISE TEST

Introduction

Sub-arctic native tribes widely used kayaks, even 4000 years ago, and the word itself originates from the inuit qajaq (man-boat). Kayak-canoe sport became a summer Olympic discipline at the 1936 Berlin games (www.olympic.org). Officially titled flatwater canoe sprint, the basic rules are simple: the fastest athlete wins. The tracks became shorter with the years, hence improving the sport performance of kayak- canoe athletes became a complex task, optimally carried out by an expert team. Each team member receives different performance feedback, which can be provided by various sensors and measurement devices. Their subjective observations supplemented by the objective data from different measurements might provide enough information for the coach regarding the optimal training strategy of the individual athletes. Despite the need for easy to understand metrics and visualization methods for improving kayakers' performance, the literature is sparse in papers describing multimodal, integrated quantitative, and visualization tools.

In sprint kayaking leg, pelvis, and trunk movements are essential for performance (Bjerkefors, Rosén, Tarassova, & Arndt, 2019). In this seminal study, they reported significant positive correlations between power output and peak shoulder and trunk flexion, trunk and pelvis rotation motion ranges, and hip, knee, and ankle flexion motion ranges. Using kayak ergometer data, others reported a high correlation between the summation of maximal voluntary contraction scores of 7 different tasks and the measured 200m performance times on the water (Steeves et al., 2019). Others reported the importance of high force output changes to high power output in long-distance kayakers (Borges, Dascombe, Bullock, & Coutts, 2015). Paddle instrumentation was utilized to investigate blade/water interactions (R.J.N. Helmer). These all support the fact that there is a need for assisting technologies for efficiently planning competition and training strategies. The training should prepare athletes to have the ability to perform at the highest level in each phase of the track (e.g., start phase, mid-race/travel phase, running-in phase). To achieve the aimed performance, continuous and instant feedback is useful for athletes to follow the instructions.

Several earlier reports showed the feasibility and reproducibility of various measurements during training (Fleming, Donne, Fletcher, & Mahony, 2012; Tay & Kong, 2018; Vadai G., 2013), in laboratory environments and on-water (Bjerkefors et al., 2019; Steeves et al., 2019; Vadai, 2013; Winchcombe, Binnie, Doyle, Hogan, & Peeling, 2019). However, sophisticated parallel data collecting, processing, and feedback systems still need to be established for kayakers.

To improve athletes' performance, we aimed to develop and test a system where biomechanical and rowing force data are collected and processed simultaneously during cardiovascular endurance training. This paper focuses on simultaneous rowing force and EMG data processing and visualization methods, which we can integrate into a complete platform for detailed comparative performance analysis.

Methods

Twelve top kayakers participated in the study (12 men, age: $23,50 \pm 3,33$ years; height: $184,21 \pm 4,09$ cm; weight: $83,00 \pm 7,17$ kg). Right, and left-handed athletes proportion was 11:1, while right and left shaft rotators were 10:2.

Subjects were top kayakers (two marathon distance, four medium (1000m), six short (200-500m) distance), and we carried out measurements with a kayak ergometer (Polaritas-GM Ltd., Budapest, Hungary)(Figure 1C.). All participants submitted their written informed consent according to the approved medical study protocol.

We examined athletes according to the provisions of the Helsinki Declaration on Human Studies, which was authorized by the Ethics Committee of the University of Physical Education (TE-KEB/No15/2018) and the Semmelweis University (205-5/2007).

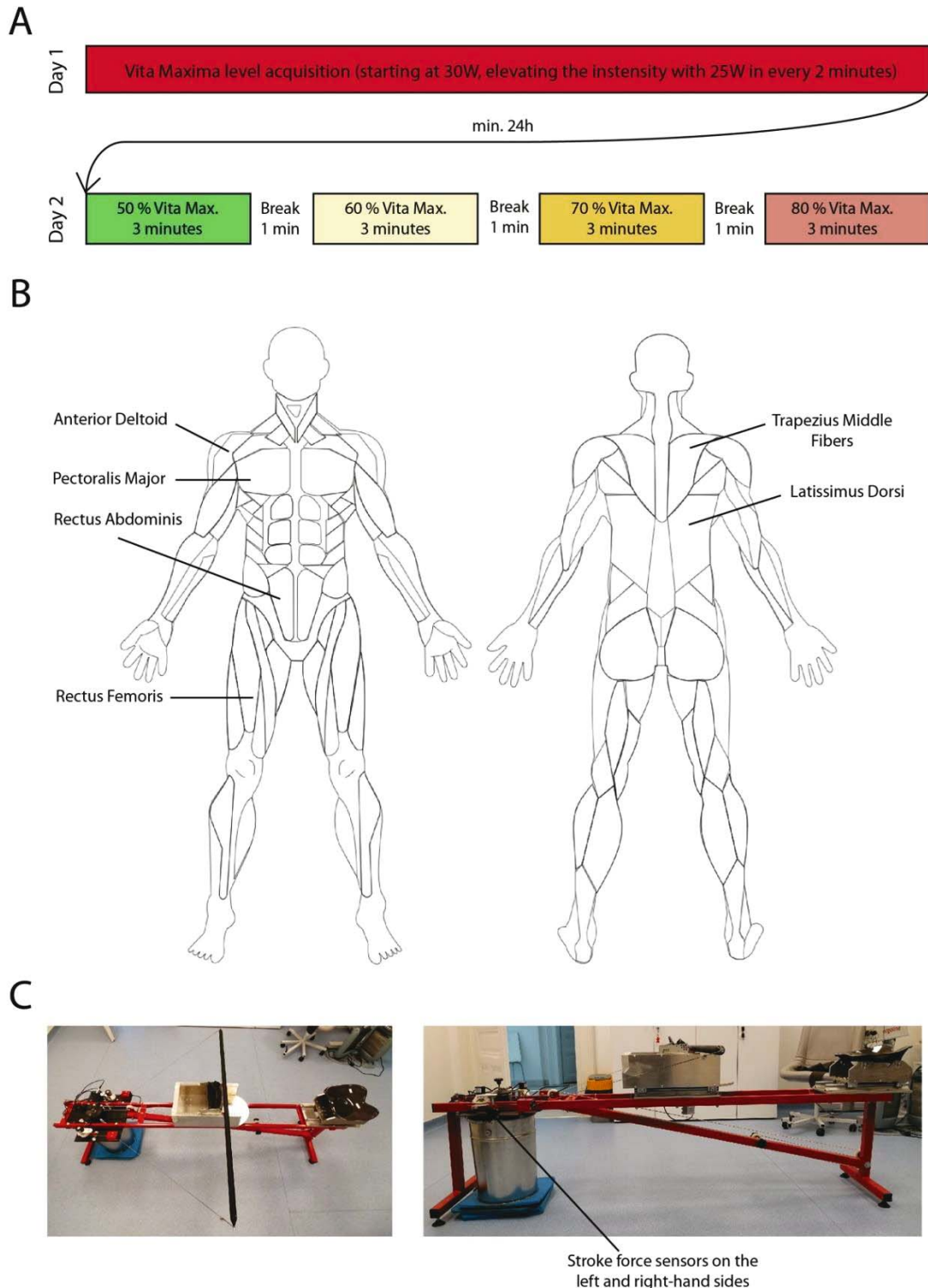


Figure 1. We carried out the testing protocol on two consecutive days with details shown on A. EMG recordings (left, right) were acquired from the muscle groups represented on B. The used ergometer with stroke force sensors installed (C).

Before the actual recording sessions, as a preprocessing protocol, a sync signal was transmitted to each recording device.

We used the left and right-hand data received from the force sensors on the ergometer to define the stroke boundaries in the paddling process. A single-sided stroke start point was when the force exceeded 12N, and the finish point was when the cycle on the other side started. We applied these boundaries to each signal consistently after synchronization. For achieving a standard frequency rate of 1kHz, we resampled data with linear interpolation.

We acquired surface EMG signals from various muscles (abbreviated rt - right, lt - left, Lat. Dorsi - m. latissimus dorsi, Middle Trap. - m. trapezius (middle fibers, transverse of the trapezius), Ant. Deltoid - m. deltoideus anterior (anterior deltoids), Pect. Major - m. pectoralis major, Ext. Oblique - m. obliquus externus abdominis, Rectus Fem. - m. rectus femoris) of the participants during exercise with the Telemyo Mini 8/16 EMG system and Skintact F55 unipolar surface electrodes (Figure 1B.). We used Noraxon's MyoResearch Master Edition software for signal registration and data processing.

According to the SENIAM international protocol recommendations, we placed the surface electrodes on the muscle between the tendon and the motor point. As various artifacts contaminated our EMG signals, we performed filtering and other methods to clarify the EMG signal. We selected 20 Hz as the low component of the applied bandpass filter to filter out movement artifacts caused by the movement of cables or electrodes. We used a notch filter for clarifying the AC line noise (50 Hz). We set the high component of the bandpass filter to 350 Hz for canceling fast oscillations due to unwanted electrical noise. According to the reasons mentioned above, the EMG signals had the most significant spectral power in the frequency range between 20-350 Hz. After applying the filters (4th-order Butterworth, notch filter), we carried out rectification and smoothing. In some cases (BP28), we experienced measurement error with the EMG electrode that monitored the left Rectus Abdom. We have removed this athlete from further analysis.

We calculated the root mean squared error (RMS) by applying a moving average window (100ms) on the signal for generating an amplitude envelope.

The exercise test began with a maximal exercise stress test (vita maxima protocol) to determine the individual's anaerobic threshold (Figure 1A.). We acquired the vita maxima level by asking the athlete to paddle with a pleasant activity starting from 30 Watts, then elevating the intensity with 25 Watts in every two minutes until total exhaustion to determine the load capacity and anaerobic threshold of the individual. We then assessed the maximum stroke power which the athletes reached during vita maxima. After 24 hours, athletes had to perform the incremental exercise test protocol (50-60-70-80% of maximum stroke power) again, while we recorded stroke force, power, and EMG simultaneously. The second test was a stepwise protocol, a standard kayak track was modelled, the athletes had to paddle 4 runs with increasing intensity, with one-minute rest between the runs. An intensity of 80% in the final stage can be equated to a competitive situation. This load profile aimed to eliminate anomalies resulting from individual differences in metabolic background and produce physical stress that may be considered equal for all participants. We sampled serum lactic acid levels during the exercise. To determine the level of "vita maxima", the conventional spiroergometric criterion system was used in addition to the maximum performance:

- maximal exercise heart rate should be $220 - \text{age}$ (1/min; Schiller CS200)
- the duration of the increasing load should be at least 5-6 minutes
- Arterial blood pH should be 7.25 or less
- RER value ($\text{RER} = \text{CO}_2 / \text{O}_2$) should be 1.0 or more (Ganshorn PowerCube)

- By increasing the load, the oxygen consumption reaches its maximum value (VO₂ curve in plateau or descending phase, VO₂max).

Having gathered all the data simultaneously, we used Python 3 programming environment for the data analysis pipeline on a dedicated server. We used pandas for data processing and scipy for filter creation and application. Those are scientific data manipulation libraries used extensively in research.

We have discussed the raw signal processing and acquisition steps above together with the EMG related postprocessing technique. We used the resulting EMG amplitude envelope to measure the intensity of the muscle. When referred to as average intensity during a stroke or tempo, we transformed this intensity by taking the arithmetic mean of all measurements in the stroke or tempo's timeframe.

Similarly to this, the output power is post-processed in this way when we observe the athlete's output power for one stroke or tempo. Before this step, however, we normalized the strokes. We have taken the maximum output power measured for the athlete for one entire stroke and used this value to max-normalize the athlete's power readings. By doing it meant dividing the instantaneous readings with the vitamax value. When we refer to the normalized average power, we simply mean the arithmetic mean of the readings during the stroke or tempo's timeframe. In later sections, we will use statistical methods like standard deviation, arithmetic mean, correlation to measure dependencies and centralities of the data while describing the EMG intensities and output power, or coactivation. We included the used equations in the Appendix section.

Results

Establishing diagnostic figures and metrics help us to assess how well an athlete can complete specific tasks. Figures offer visual cues to understand the behavior of the athlete over time or other dimensions. Metrics are condensed forms of some measurements that can make a fair comparison between athletes; for instance, how far an athlete can run in 10 minutes or how much weight an athlete can lift. Through supervised settings, one can obtain various measurements via computer-aided diagnostic environments. These measurements can be fed into algorithms to provide metrics about the smallest details of the athlete's performance.

While studying target output differences, figures we describe in this section helped us to diagnose the athlete's ability to complete the task and to give informative results where he could improve technique, stamina, or power. For each athlete, we recorded four runs intending to maintain a steady 50, 60, 70, and 80% normalized power output measured on the ergometer. We recorded normalized power 24h before when we measured the theoretical maximum output power for each athlete.

Figure 2 shows the normalized output power measured on the ergometer over time, with the first and the last ten tempos (left-right strokes) removed. Run 0, 1, 2, and 3 depicted by different colors show the normalized output power (50, 60, 70, and 80%). With this method, it is easy to show that each athlete had a different success of being able to reach and maintain the power output at a steady level for the task. Spikes (both in the upward and the downward direction), up- or down trends show fatigue or loss of momentum. Athletes received direct feedback about their actual normalized power values on a display to know if they are under- or overperforming (Figure 2.). To measure and diagnose the correctness of completing the task, one can take the arithmetic mean of the normalized output power for different runs and subtract the goal of 50-80% for each run to measure if the athlete under- or overperformed on the task. On average the measured athletes were unable to reach the goal normalized output powers by 2.32% for the 1st

run (50%), 2.9% for the 2nd run (60%), 3.95% on the 3rd run (70%) and 4.01% on the 4th run (80%), which means that it is increasingly harder to achieve the goal as the output power requirement increases.

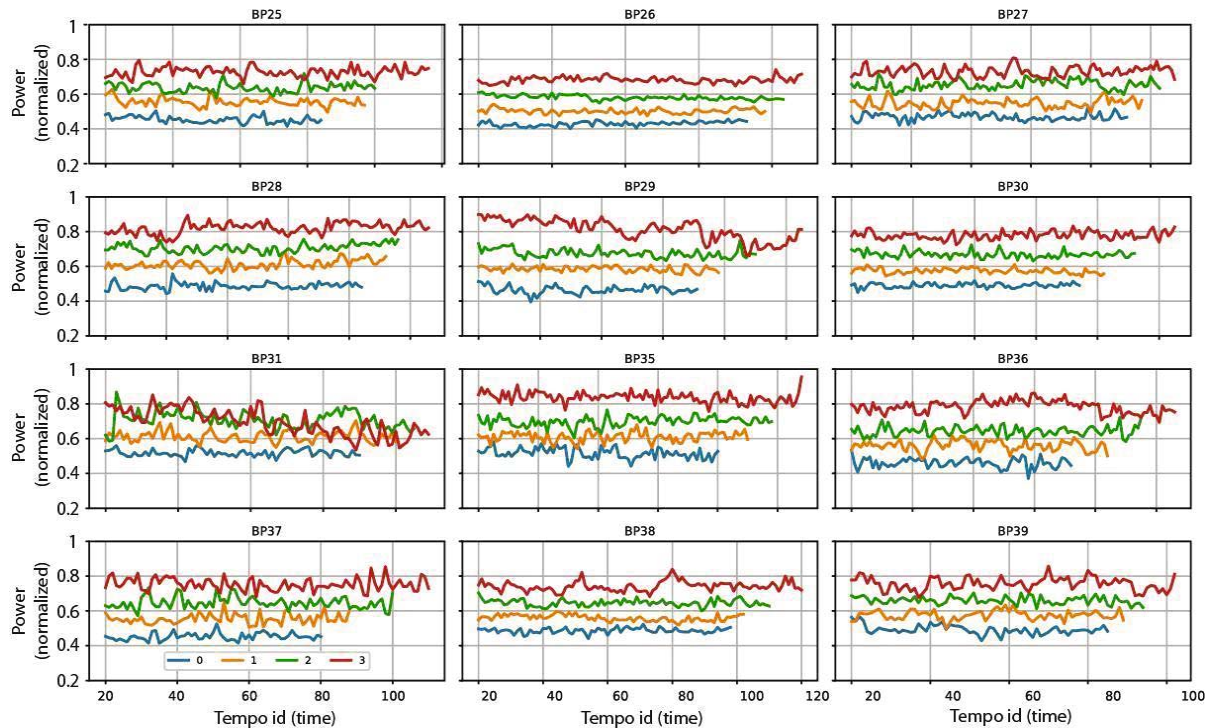


Figure 2. 12 athletes' normalized output power (y-axis) measured on the ergometer over time (x-axis), with the first and the last ten tempos (left-right strokes) removed. Run 0, 1, 2, and 3 plotted with different colors (blue, orange, green, red) show the variation of the normalized output power (50, 60, 70, and 80%). One unit on the x-scale represents 20 tempos in all cases.

One can take the arithmetic mean of the differences of the normalized power outputs and the goals for each athlete for each run. Next, one can calculate the average of those four values. Negative values characterize underperforming; positive values mean overperforming athletes. We observed that reaching the power requirement was increasingly complicated for athletes as they approached 100% of the theoretical normalized output (*vita maxima*). Maintaining the required level for the 50% task is less complicated than the same for the 80% task. For compensation, one can employ a weighting scheme for the average differences with linearly increasing weights given to the more laborious task. Alternatively, one can apply other increasing schemes, for instance, quadratic or exponential scenarios. Quadratic and exponential weights emphasize the harder to achieve tasks. For instance, the 80% normalized power output goal is weighted 64% in the exponential scheme, while weighted only 31% in the linear case, the quadratic lies in the middle with 53%. The weights are normalized so that they add up to 1.0. After following this strategy, we only had to multiply the goal to actual performance differences of individuals with the corresponding weight and sum up for the four runs to get the correctness score of an athlete (Table 1).

Various weighting schemes provide different overall ranking of the athletes because they penalize for different errors. Table 2. summarizes scores and the corresponding ranking of the participating athletes sorted by the linear weighting scheme. The first four and the last two ranks are the same for all weighting schemes—the ranking changes in the middle with athlete BP31 having the wildest swings in the ranking. From the Figure showing the power output time series (Figure 2), one can identify that the subject (BP31) ran out of stamina and could not complete the 80% run. Downward trend characterized the normalized output power, and this behavior

returned for the same athlete in the 70% target run. The quadratic weighting of the mean difference penalizes BP31 more and lifts others (BP36, BP37), who were able to perform the most laborious part better.

Normalized power	Linear weight	Quadratic weight	Exponential weight
50%	0.19	0.03	0.03
60%	0.23	0.13	0.09
70%	0.27	0.31	0.24
80%	0.31	0.53	0.64

Table 1. Different weighting schemes for the normalized output power

Id	Lin. rank	Quad. rank	Exp. rank	Lin weight.	Quad. weight.	Exp. Weigh.
BP35	1	1	1	1.72	2.19	2.56
BP28	2	2	2	0.80	1.36	1.49
BP29	3	3	3	-1.35	-0.47	-0.11
BP30	4	4	4	-2.28	-2.44	-2.35
BP31	5	8	10	-2.34	-5.07	-6.35
BP39	6	6	6	-3.12	-3.87	-4.00
BP36	7	5	5	-3.68	-3.21	-2.85
BP38	8	9	8	-4.42	-5.31	-5.43
BP37	9	7	7	-4.82	-4.84	-4.81
BP27	10	10	9	-5.21	-5.92	-6.15
BP25	11	11	11	-5.83	-6.50	-6.70
BP26	12	12	12	-10.41	-11.37	-11.46

Table 2. Ranking of the athletes by the weighted correctness score ($w_{_}$)

In general, the proposed metric for power output measurement is the arithmetic mean difference between the goal power output and the observed power output. With different weighting and penalizing strategies, it is possible to find individualized solutions for helping athletes.

The variability of the normalized power outputs, which depicts the athletes' movement's fluidity, can be measured by the standard deviation of each run. Low standard deviation refers to a set of output power measurements dispersed closer to the mean, while a higher standard deviation means the measurement points are farther away from the mean on average (Table 3.). As with the previous metric Figure 2 shows the power outputs for each run for 50-80% targets. According to the previous results, we obtained the standard deviations for each athlete and took the

arithmetic mean for each run (12 standard deviations for each run). Results show that the standard deviation increases as the target power output rises, meaning it is harder to maintain the fluidity of movement and the constant rate of power output when the target output is higher. On average for the 12 athletes tested, the average standard deviation was 0.02 for the normalized power outputs for the 1st run (50% target output), 0.023 for the 2nd run (60% target output), 0.26 for the 3rd run (70% target output) and 0.36 for the last 4th run (80% target output). Similar weighting schemes may be applied, as shown previously in Table 1, with increasing weights given to more laborious tasks (more considerable target output power). The standard deviations calculated from the normalized power are directly comparable to the previous setting. The theoretical minimum of this metric, which is 0.0, represents the athlete's constant output power generation.

Id	Lin. rank	Quad. rank	Exp. rank	Lin weight.	Quad. weight.	Exp. Weigh.
BP26	1	1	1	1.48	1.57	1.61
BP30	2	2	2	1.85	2.08	2.15
BP38	3	3	3	2.09	2.38	2.49
BP25	4	4	4	2.5	2.66	2.69
BP27	5	5	5	2.61	2.78	2.82
BP28	6	6	6	2.62	2.86	2.93
BP39	7	8	8	2.87	3.09	3.24
BP35	8	7	7	2.95	2.97	3.01
BP36	9	9	9	3.1	3.28	3.37
BP37	10	10	10	3.14	3.44	3.48
BP29	11	11	11	3.3	4.22	4.65
BP31	12	12	12	4.84	6.11	6.49

Table 3. Movement fluidity based on the variability of power output and athlete rankings with different weighting schemes

In general, the closer the standard deviation is to 0.0, the better the athlete maintains the pace and the output power. In Table 3, one can observe that the different weighting schemes do not significantly change the overall ranking of the athletes. If we do not apply weighting at all, the ranking is almost identical to the linear rank, with only one position change. This metric captures the information content of a massive downward trend observed at BP31 and BP29. Additionally, it correctly observes the high fluidity of movement level of athletes BP26 and BP30. Our measurements suggest that the most efficient method of analyzing the fluidity of output power is calculating the standard deviation of the normalized output power. In this case, one can compare the performances of athletes directly if there is a single target output power goal to reach. Alternatively, one can calculate the average of all standard deviations in each run to draw results for the training session. A weighting scheme seems unnecessary complication in this case.

For each stroke and tempo, we can summarize the output power and measure the overall time to finish one stroke or tempo. The latter is described as tempo duration and plotted in Figure 3 for the 12 athletes. This representation method shows that increasing target output power results in a tempo length decrease for almost all athletes. There is a strong negative correlation (-0.681) between the normalized output power for each tempo and the output power, meaning that a more massive normalized output is associated with a shorter tempo duration (Figure 4).

Figure 3 shows that athlete BP31 was unable to reach and maintain the 80% target output power and was unable to decrease the tempo duration any further. It is also present to some extent in tempo duration data of athlete BP27 for the last two output targets (70 and 80%). Interestingly for BP27, output power differences of the last two output targets in Figure 2 are more significant than observed in the case of BP31. It could mean that the athlete achieves the output power difference by not decreasing the tempo duration but using his muscles differently or more intensely for completing the task. One might need to use information unveiled with these methods for finding the most optimal training and competition tactics.

We have found that the range of tempo duration differences across target outputs (50-60-70-80%) is characteristic of athletes. Athlete BP26, BP27, BP28, and BP38 had only a 200 ms full tempo duration window across target outputs, while BP36, BP37, BP29 had more than 300 ms windows. Athletes with lower ranges were generally the least successful in achieving the required target outputs. However, we cannot generalize in the other direction: a more extensive duration range does not necessarily mean better performance in reaching the output target (Figure 3).

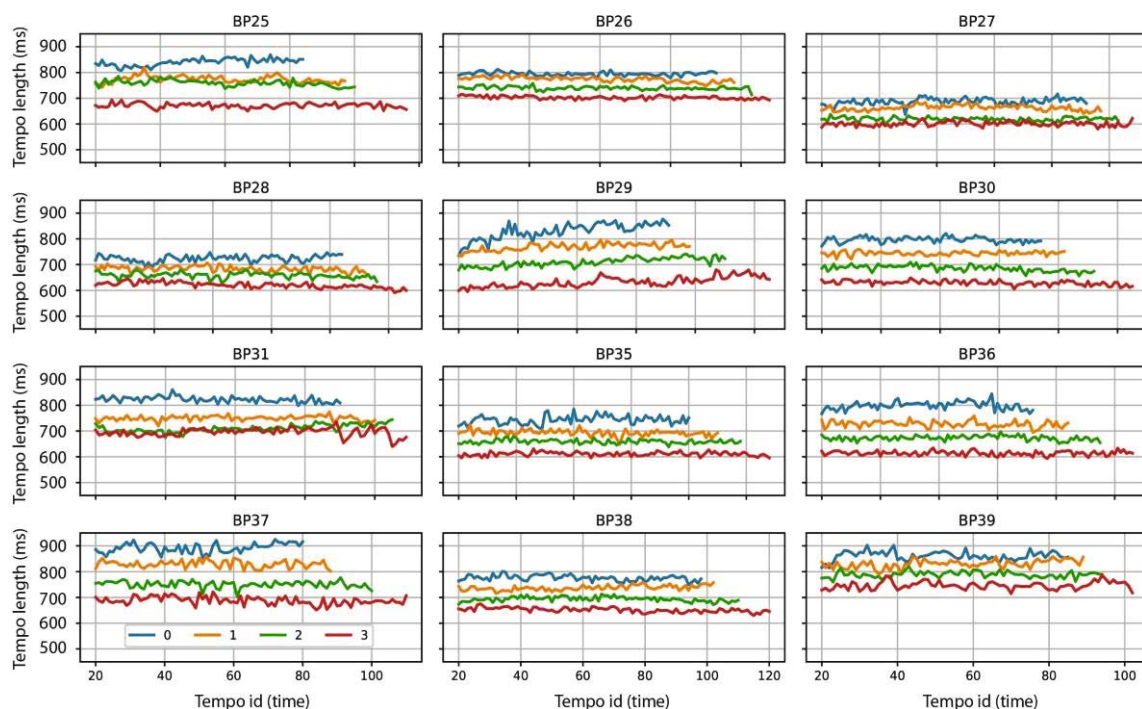


Figure 3. Tempo duration over time (tempo id) for 12 athletes. Run 0, 1, 2, and 3 plotted with different colors (blue, orange, green, red) show the variation of the normalized output power (50, 60, 70, and 80%). For each stroke and tempo, we can summarize the output power and measure the overall time to finish one stroke or tempo. This representation method shows that increasing target output power results in a tempo length decrease for almost all athletes. One unit on the x-scale represents 20 tempos in all cases.

Our next task was to understand the relationships between muscle intensity and output power. Figure 5 shows the 5th to 9th tempos of athlete BP26 on 80% target power output (1st subplot) and the six combined muscle activity intensities that we collected throughout the observation

period for each athlete (2nd-7th subplot). This example shows various muscle activity characteristics of kayaking through left and right-handed strokes. Orange color denotes the muscle intensity related to the right side for respective muscles, and green shows the left side. There is also a third blue line, which denotes the activity threshold as 0.1 (10%) of all the normalized muscle intensities for that specific muscle group. Above the 10% threshold, we considered the muscle active. One peak in output power is considered a stroke, and two consecutive left-right strokes constitute a tempo.

In Figure 5, one can observe a periodic signal in the output power and some of the muscles (Lat. Dorsi, Middle Trap., Pect. Major, Rectus Abdom.). However, this periodic nature is not that present in Rectus Fem., and Ant. Deltoid. Rectus Fem. muscles are considered inactive through the majority of the time during the example period shown in Figure 5. From the periodically active muscles, Lat. Dorsi, Middle Trap., and Pect. Major are single-sided, meaning that only one side of the given muscle type contributes to activity during a stroke. As we divided each tempo into a left and a right stroke, we can observe that for a left stroke left Lat. Dorsi and left Middle Trap., Pect. Major are active.

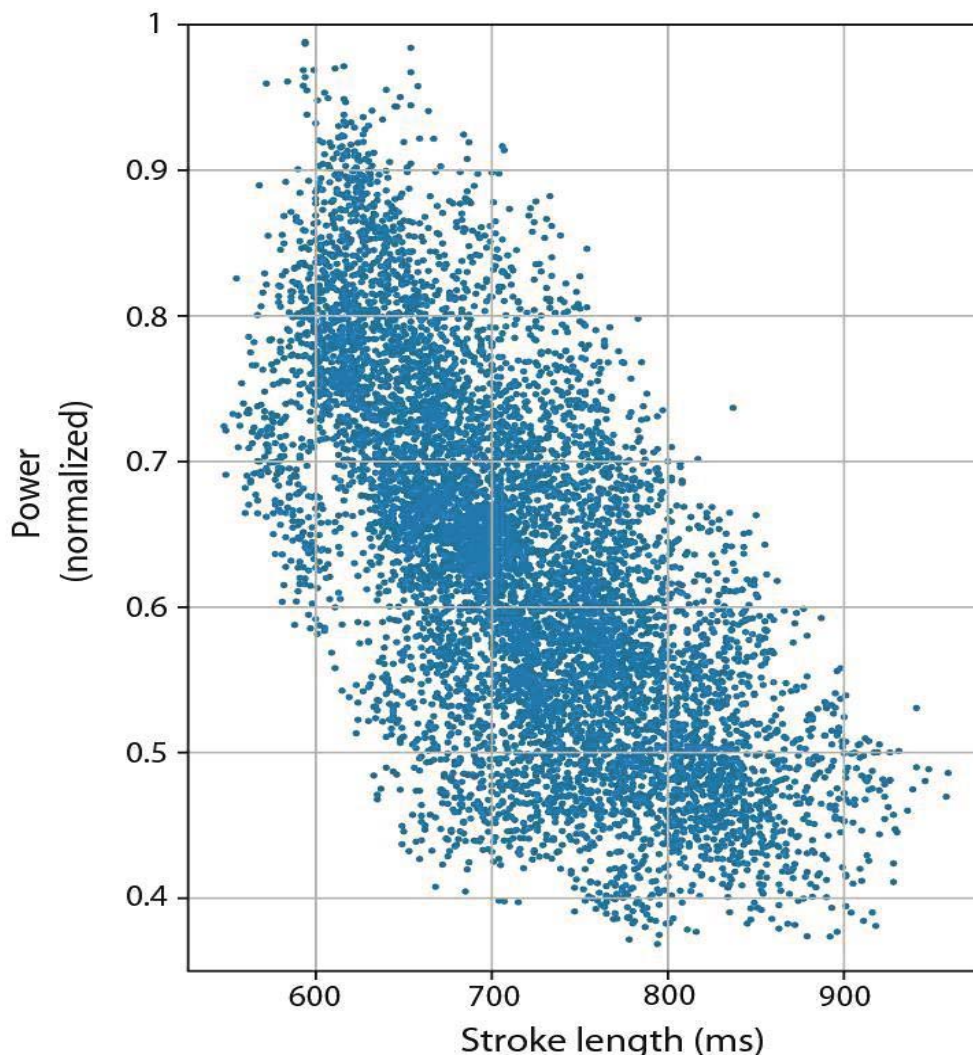


Figure 4. There is a strong negative correlation (-0.681) between the normalized output power for each tempo and the output power, meaning that a more massive normalized output is associated with a shorter tempo duration.

Similarly, for a right stroke right, Lat. Dorsi, right Middle Trap. and the left Pect. Major muscles are active. For the Rectus Abdom. being a periodic signal itself, both sides of this muscle group

get activated during each stroke.

Tables 4 and 5 summarizes the periodic muscle activities for each side of the stroke. One can observe that Lat. Dorsi and Middle Trap. behave similarly, as demonstrated in Figure 5. Stroke side muscle activities are more active (measured by the average activity throughout the stroke); however, for Pect. Major, this is not the case for all athletes tested. Some athletes show increased activity on the same side, similar to Lat. Dorsi and Middle Trap. (BP29, BP35, and BP27).

Additionally, activity differences in the case of Pect. Major are not that significant as with the other two muscles. It could mean they have a different style or a systematic error in the use of the muscles. Athletes BP29 and BP35 are both classified as 2nd grade based on the results they were having assumed by a respected coach. In conclusion, this result suggests that they should improve muscle coordination to be similar to the others, which may lead to better results on the ergometer and the field (at least for this particular set of muscles).

muscle	LT LAT.DORSI		LT MIDDLE TRAP.		LT PECT. MAJOR	
Stroke type	L	R	L	R	L	R
Id						
BP25	0.1807	0.0915	0.2414	0.0754	0.0801	0.1145
BP26	0.1505	0.0938	0.1369	0.1317	0.0385	0.0398
BP27	0.1459	0.0366	0.2011	0.0990	0.0550	0.0659
BP28	0.2071	0.0526	0.1997	0.0901	0.0822	0.1638
BP29	0.1880	0.0608	0.2086	0.0983	0.0723	0.0670
BP30	0.1590	0.0698	0.1774	0.1380	0.0265	0.0642
BP31	0.1525	0.0575	0.2322	0.1172	0.0531	0.1070
BP35	0.2252	0.0385	0.2474	0.1067	0.1072	0.0460
BP36	0.1746	0.0627	0.2410	0.1436	0.0647	0.0810
BP37	0.1690	0.0625	0.3069	0.0844	0.0627	0.0787
BP38	0.1935	0.0563	0.2008	0.1506	0.0645	0.0930
BP39	0.1663	0.0852	0.2295	0.1843	0.0459	0.1561

Table. 4. Average left-side periodic muscle intensities per stroke and athletes.

Muscle	RT LAT.DORSI		RT MIDDLE TRAP.		RT PECT. MAJOR	
Stroke type	L	R	L	R	L	R
Id						
BP25	0.0667	0.1581	0.0614	0.2128	0.1022	0.0685
BP26	0.0669	0.1574	0.1422	0.2775	0.0629	0.0426
BP27	0.0453	0.1791	0.0983	0.1880	0.0502	0.0541
BP28	0.0635	0.2037	0.1287	0.2687	0.1253	0.0694
BP29	0.0603	0.2007	0.1917	0.2595	0.0985	0.0483
BP30	0.0892	0.1911	0.1699	0.2077	0.0533	0.0351
BP31	0.0580	0.1577	0.0792	0.2453	0.1559	0.0693
BP35	0.0372	0.2050	0.0985	0.2473	0.0570	0.0676
BP36	0.0465	0.1468	0.1115	0.1906	0.0830	0.0342
BP37	0.0923	0.1871	0.0640	0.2257	0.1074	0.0807
BP38	0.1058	0.2062	0.1132	0.1248	0.0934	0.0479
BP39	0.0750	0.1579	0.1220	0.2810	0.1342	0.0571

Table 5. Average right-side periodic muscle intensities per stroke and athletes.

If we observe muscle activity in general (Table. 6.) aggregated by runs, we can draw a classification for those muscles that were not that obvious in the first demonstration as to what class they belong to. Table 6. shows this aggregation, where we can draw the conclusion that Ant. Deltoid, Lat. Dorsi, Middle Trap., and Rectus Fem. are more intensely active on the same side as the stroke itself, while Pect. Major and Rectus Abdom. are more active on the opposite side of the body compared to the stroke. With these results, we can conclude this is the expected behavior from athletes, and where this is not present, they might increase their output by coordinating the muscles in the right direction.

One can also observe that by increasing the output from 50 to 80% of vita maxima, we can see an increase in almost all muscle (LT Ant. Deltoid has a slight decrease in 80% vita maxima) activities, which could also be an essential observation during training. For example, if we do not see this increased activity in one particular muscle, we can warn the athlete that he needs more activity on that muscle in order to paddle correctly. The average muscle intensity difference in specific muscles (Rectus Abdom., Rectus Fem.) is not significant, which means that if the athlete performs adequately based on normalized output power but lacks the coordination in these two less distinctive muscle groups, they might not have to change the overall style. Some of our future work will focus on these muscles to study whether they significantly impact the output power or not.

	Run	0	1	2	3	
Muscle (R prefix: right side; L prefix left side)	Stroke type					Class
LT ANT.DELTOID	L	0.1491	0.1511	0.1607	0.1693	
	R	0.1174	0.1259	0.1331	0.1271	same side
LT LAT.DORSI	L	0.1499	0.1690	0.1815	0.2019	
	R	0.0548	0.0608	0.0657	0.0722	same side
LT MIDDLE TRAP.	L	0.2096	0.2140	0.2236	0.2251	
	R	0.0983	0.1091	0.1235	0.1394	same side
LT PECT. MAJOR	L	0.0470	0.0569	0.0669	0.0792	
	R	0.0689	0.0808	0.0929	0.1121	opposite side
LT RECT.ABDOM.LO.	L	0.0428	0.0480	0.0547	0.0647	
	R	0.0521	0.0566	0.0675	0.0794	opposite side
LT RECTUS FEM.	L	0.0356	0.0421	0.0434	0.0480	
	R	0.0335	0.0394	0.0395	0.0437	same side
RT ANT.DELTOID	L	0.1407	0.1505	0.1544	0.1561	
	R	0.1554	0.1625	0.1707	0.1812	same side
RT LAT.DORSI	L	0.0583	0.0635	0.0693	0.0761	
	R	0.1577	0.1704	0.1854	0.2028	same side
RT MIDDLE TRAP.	L	0.0956	0.1045	0.1200	0.1387	
	R	0.2123	0.2221	0.2317	0.2411	same side
RT PECT. MAJOR,uV PROC	L	0.0674	0.0833	0.1006	0.1193	
	R	0.0406	0.0492	0.0613	0.0716	opposite side
RT RECT.ABDOM.LO.	L	0.0562	0.0663	0.0800	0.0898	
	R	0.0477	0.0549	0.0596	0.0661	opposite side
RT RECTUS FEM.	L	0.0423	0.0456	0.0475	0.0497	
	R	0.0578	0.0552	0.0570	0.0616	same side

Table 6. Classification of muscle activities in general based on their activation patterns during runs

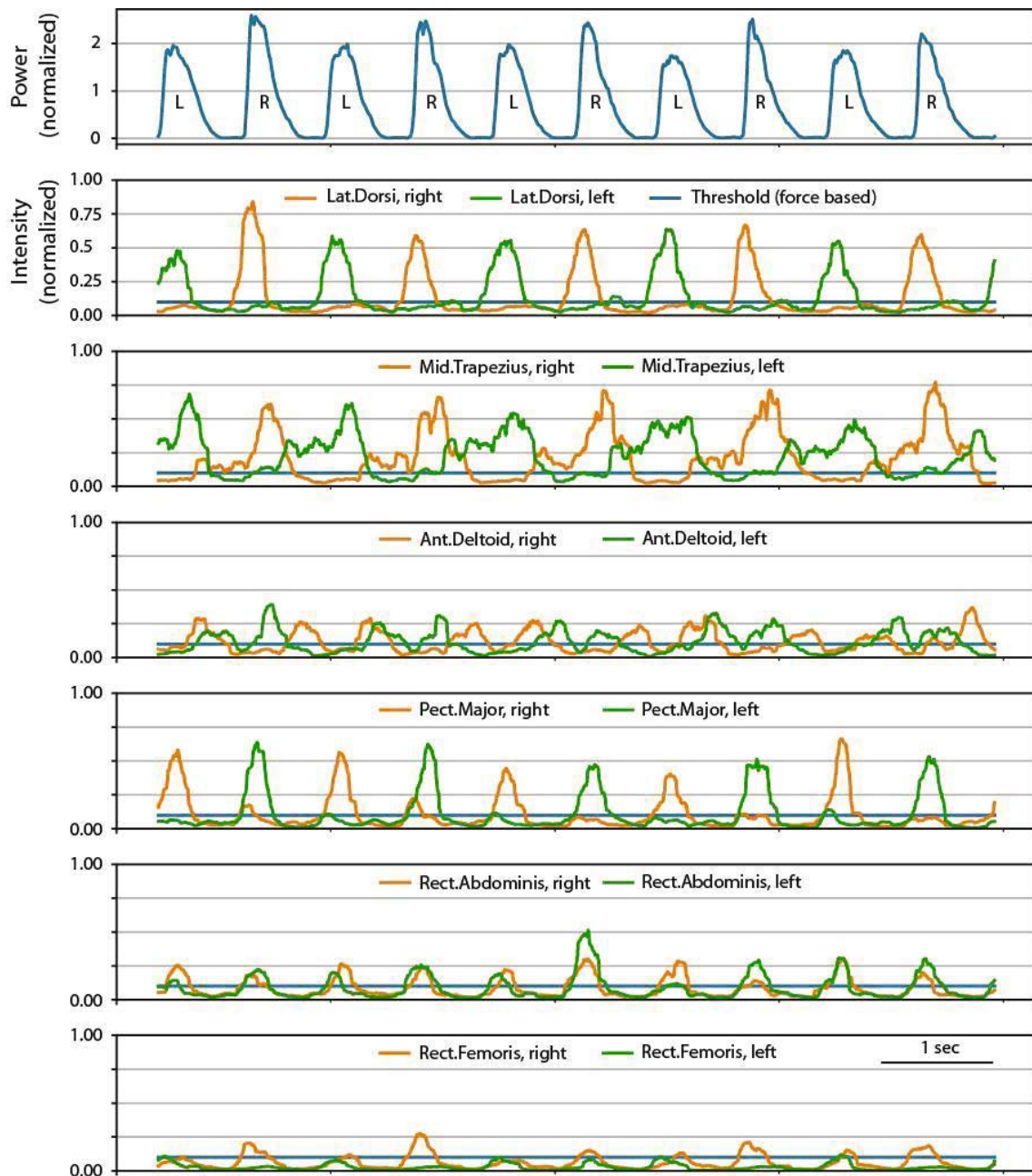


Figure 5. Relationships between muscle intensity and output power. Tempos 5th to 9th of athlete BP26 on 80% target power output (1st subplot) and the six combined muscle activity intensities that we collected throughout the observation period for each athlete (2nd-7th subplot). Orange color denotes the muscle intensity related to the right side for respective muscles, and green shows the left side. Above the 10% threshold (blue line), we considered the muscle active. One peak in output power is considered a stroke, and two consecutive left-right strokes constitute a tempo.

We should also note that with our system, more nuanced analysis is available for each athlete. For example, lags between muscle activity peaks and the result in output power. However, this is part of the future work that we plan to accomplish.

In summary, the computational methods used in this section are simple but effective ways to measure athletes' performance in a laboratory setting. The corresponding formulae for computing the arithmetic mean, moving average, and root mean squared error is included in the appendix section.

Asymmetry

One other particular phenomenon observed from Figure 6 tempos is that athlete BP26 has an asymmetric stroke style: left strokes are generally less potent than right strokes in this example. We can consider these observations as a particular style of kayaking (Table 7.). We can calculate the power output asymmetry by taking the difference of the arithmetic mean average of the right and left strokes that occurred in a particular target output. One athlete out of the 12 has a stronger left stroke (BP38), while the others have a more robust or similar left stroke. The magnitude of the average difference throughout the measurement period depicts which athlete has this particular asymmetric style and for which side he exhibits this behavior. For example, BP37 has an average difference of 12% in normalized output power; if he were to improve the other, less capable side, he could reach more power output and perhaps more speed on the water. Some athletes do not exhibit this phenomenon and remain in a +/-3% difference range: for example, athlete BP36 has almost identical strokes in terms of output power regardless of which side the stroke occurs.

Id	50%	60%	70%	80%	Average difference
BP25	0.0383	0.0310	0.0702	0.1294	0.0753
BP26	0.0577	0.0672	0.0742	0.0682	0.0663
BP27	0.0077	0.0017	0.0231	0.0379	0.0223
BP28	0.0634	0.0549	0.0785	0.1116	0.0828
BP29	0.0178	0.0161	0.0367	0.0726	0.0371
BP30	0.0011	0.0089	0.0008	0.0343	0.0138
BP31	0.0424	0.0909	0.0857	0.1040	0.0823
BP35	0.0459	-0.0043	0.0348	0.0535	0.0419
BP36	0.0425	0.0251	0.0100	0.0003	0.0123
BP37	0.0616	0.0846	0.1329	0.1935	0.1252
BP38	-0.0070	-0.0448	-0.0497	-0.0323	-0.0330
BP39	0.0559	0.0515	0.0576	0.0528	0.0528

Table 7. Stroke asymmetries

The output power increase has a different effect on the athlete in terms of this asymmetry. In the case of BP25, BP27, BP29, and BP37 we see a definite increase in asymmetry. However, for BP36 we see a monotonic decrease. The increase means that the athlete develops more power on his strong side than on the weaker side, focusing more effort on the strong side. The decrease means that the weaker side gets more emphasis on trying to deliver the required output power. In other cases, there is no clear trend. In general, the asymmetry measure value increases as we go from the 50% target output towards the 80% target output. In the previous section, we devised a measurement scheme to obtain a score for each athlete's correctness to quantify how well they could complete the task.

In the future, we plan to analyze the significant kayaking styles better and identify effective ones

with adequate and timely muscle activity involvement.

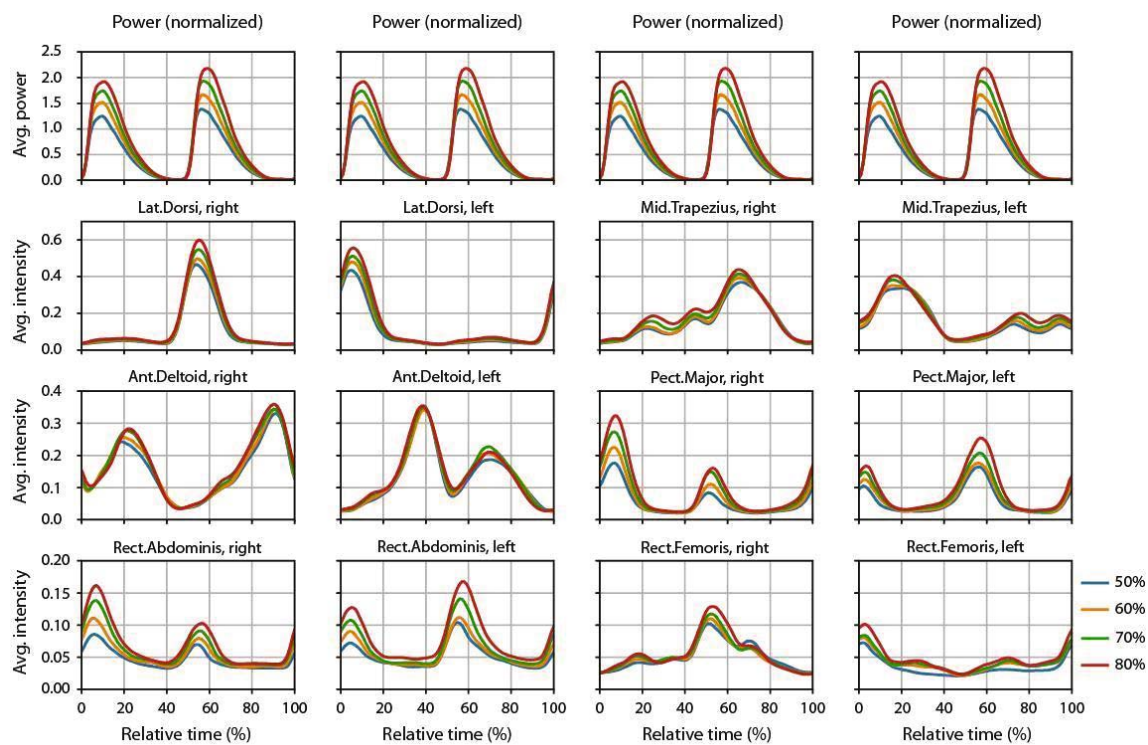


Figure 6. The time-normalized average muscle intensities for each of the four normalized target outputs of athlete BP26. We depict the general periodic behaviour of the muscles through time and the power output (first row). Based on our results, BP26 has an asymmetric stroke style: left strokes are generally less potent than right strokes. We can consider these observations as a particular style of kayaking. The asymmetry of power output throughout each output threshold can be measured by taking the difference of the average of the right and left strokes that occurred in a particular target output.

Muscle intensity vs. output power

To understand the effect a muscle intensity has on the normalized power output, we have taken all measurement samples and derived the linear correlation coefficient between the normalized output power and each muscle intensity. Correlation is a measure of the strength of a linear relationship between two quantitative variables. Positive correlation is a relationship between two variables in which both variables move the same direction, while negative correlation is a relationship where one variable increases as the other decreases. We included the used formula in the Appendix section. We selected left and right-side strokes separately because we have shown that there is a difference between activation and muscle intensity in regard to the side of the strokes. (Table 8.) While correlation does not imply causation, it is safe to assume that increased muscle intensity affects normalized power output. We observed exciting patterns, as described below:

The most significant positive correlation with normalized output power is the Lat. Dorsi muscle. The right Lat. Dorsi has a significant positive correlation (0.7119) on normalized output power for the right strokes and the left Lat. Dorsi to the left strokes (0.6751). There is a weak negative relationship with the other sides (Left Lat. Dorsi to right stroke: -0.1766, Right Lat. Dorsi to left stroke: -0.1920), respectively. Middle Trap. behaves similarly to Lat. Dorsi with a slightly lower but still strong correlation effect on the same side (Left Middle Trap. to left stroke: 0.5052, Right Middle Trap. to right stroke: 0.5742), and a slightly more negative impact on the opposite side stroke (Left Middle Trap to right stroke: -0.2738, Right Middle Trap to left stroke: -0.3321). Pect. Major, as we have seen, has its effect on the opposite side: higher intensity in the

left muscle while a right stroke increases the normalized power output (0.5425). Similarly, the increased right muscle intensity correlates with increased normalized power output on left strokes (0.5808). For the same side strokes, they do not influence the normalized power output. These three muscle groups are the most influential in defining the output power. They operate on a single side only, meaning that improving the muscles only affects one side at a time.

Muscle	Left stroke	Rght stroke
LT ANT.DELTOID,uV PROC	-0.5254	0.2271
LT LAT.DORSI,uV PROC	0.6751	-0.1766
LT MIDDLE TRAP.,uV PROC	0.5052	-0.2738
LT PECT. MAJOR,uV PROC	0.0184	0.5425
LT RECT.ABDOM.LO.,uV PROC	0.3139	0.4929
LT RECTUS FEM.,uV PROC	0.2341	-0.0995
RT ANT.DELTOID,uV PROC	0.1549	-0.5472
RT LAT.DORSI,uV PROC	-0.1920	0.7119
RT MIDDLE TRAP.,uV PROC	-0.3321	0.5742
RT PECT. MAJOR,uV PROC	0.5808	0.0965
RT RECT.ABDOM.LO.,uV PROC	0.5252	0.3644
RT RECTUS FEM.,uV PROC	-0.1288	0.3429

Table 8. Muscle intensity (EMG) and output power correlation.

Interestingly Ant. Deltoid has a robust negative effect on normalized output power for the same side stroke (Left stroke: -0.5254, Right stroke: -0.5472) and has a little positive effect on the opposite side stroke (Left stroke: 0.1549, Right stroke: 0.2271). This muscle group hinders the normalized output more than it provides an increase.

The most exciting muscle group is Rectus Abdom. in these terms, as it provides a moderate and robust effect on normalized power output on both sides (Left muscle to left stroke: 0.3139, Left muscle to right stroke: 0.4929, Right muscle to left stroke: 0.5252, Right muscle to right stroke: 0.3644). Therefore, increasing the capabilities and control of this muscle group may result in increased normalized output. The muscle group reflects the idea of holding the torso steady for each stroke in order to perform the pedaling motion correctly.

In order to study the general periodic behavior of the muscles over time, we computed time-normalized average muscle intensities for each of the four normalized target outputs (Figure 6). We can observe the ever-increasing muscle intensity for all four target normalized outputs. Lat. Dorsi has a lag: the peak intensity precedes peak output power and is the most intensely used muscle. Rectus Fem. generally follows the curve of Lat. Dorsi, while on average, has significantly lower intensity values. Rectus Fem. seems to be multimodal, peaking at different points in relative time: the maximum value for the left muscle at 0-5% of the stroke length during the left stroke phase a smaller local maximum at 30% and 70% relative time. The same is true for the right muscle: during the right stroke phase starting point, the maximum intensity is

reached. Next, at 70% relative time, there is a local maximum and another at 15-20%. One can note that local maximums are both below 0.1 relative intensity, which is considered muscle inactivity.

Pect. Major is also multimodal in the sense that the left muscle is at maximum during the right stroke phase, and there is a local maximum at the same relative time during the start of the left stroke phase. Interestingly Ant. Deltoid muscles do not observe that significant difference between target outputs—the intensity for the right muscle peaks after the right Lat. Dorsi muscle, almost at 90% relative time, followed by a local maximum during the end of the left stroke phase at around 20%. A local minimum is reached precisely at the point where the right stroke starts to gain power. The same is true for the left muscle; one can observe a peak intensity value after the peak value of left Lat. Dorsi (at around 40% of the tempo, end of the left stroke), followed by a local maximum during the right stroke phase at around 70% total normalized time.

Rectus Abdom. LO. follows similar characteristics as Pect. Major at the same normalized times, although at around half the intensity as Pect. Major.

Middle Trap. muscles maximum intensity is reached during the same stroke phase as the side of the muscle. These muscles have the longest time when they are active. There is a new waveform during the opposite side strokes with two distinct local maxima after the stroke's power starts to decline, which would need further investigation in future studies.

In conclusion, we can observe that muscle usage patterns are characteristics of individuals. Furthermore, we can identify an individual's weaknesses in specific muscle strength compared to the athletes' overall samples. As soon as we identify clusters based on anatomical features and performance categories, we can advise on training strategy based on the individuals' muscle pattern.

Coactivation

The last chapter offers some insights that there are muscles that are active concurrently; this phenomenon is called coactivation. To measure coactivation, we set a 10% activation threshold for each muscle.

Figure 7 shows the coactivation of different muscles for 70% normalized target output. The characteristics of coactivation do not change at different levels of the target output, The coactivation ratio increases slightly, but no new muscle combinations get activated as the target output increases.

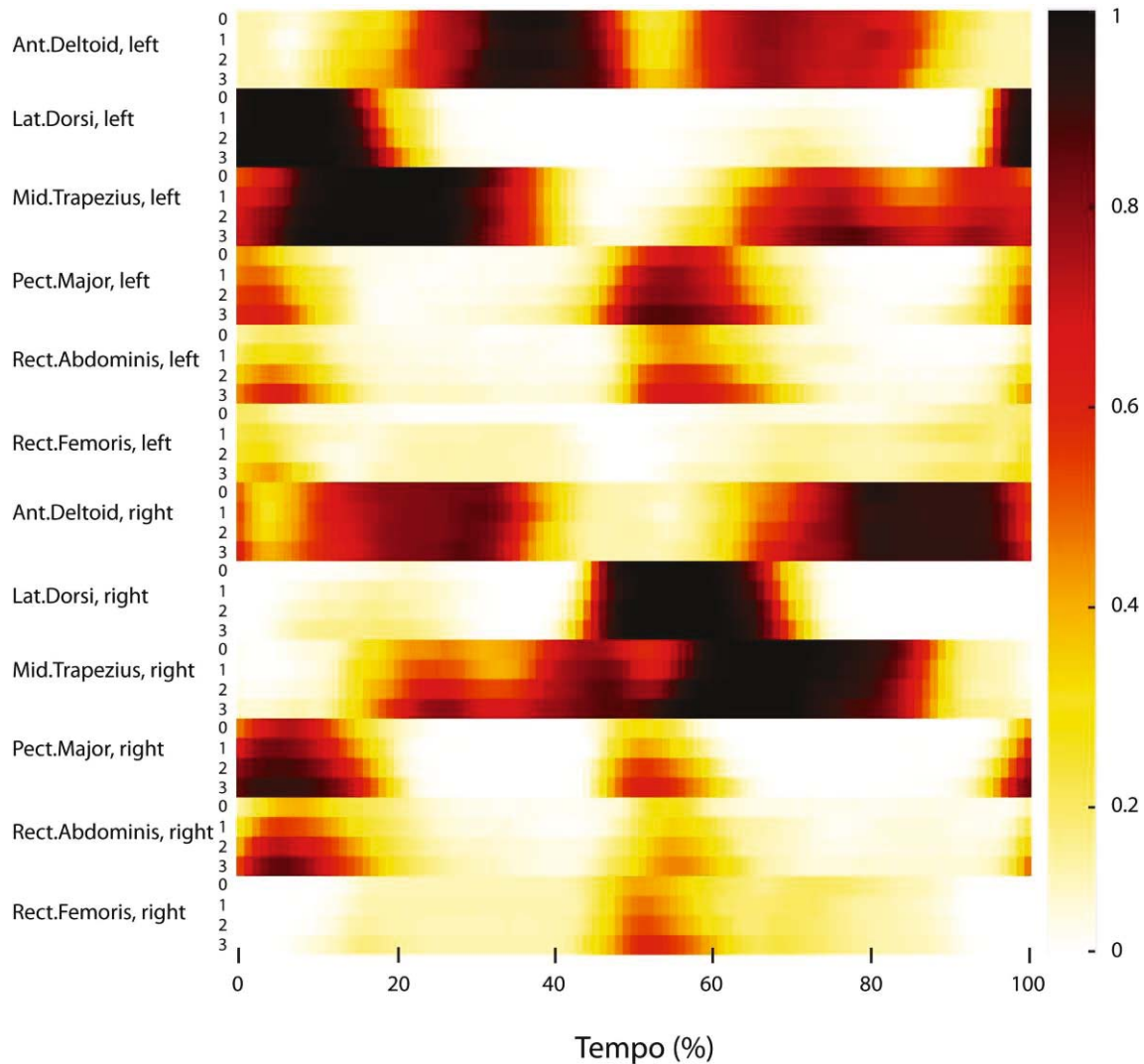


Figure 7. Coactivation of different muscles for 50-60-70-80% normalized target output for the period of an entire tempo (x-axis). Muscle groups and runs (0,1,2,3) are depicted on the y-axis. The coactivation rate of 2 muscles is high (black) when they are active at the same time and low (white) when they are inactive. The x-axis represents the percentage of the total tempo time. The color bar on the right codes the coactivation level (0-1).

Figure 8 shows the overall coactivation percentage of different muscles. The diagonal of the matrix shows the average activity for each muscle. The most active muscles are the left and right Ant. Deltoid (51% and 56% overall average activity) and left and right Middle Trap. followed by left and right Lat. Dorsi and left and right Pect. Major.

As for the coactivation, there are only a handful of combinations where we can observe strong coactivation intensities, which we can measure here by counting the samples where the muscles were active together, divided by all measured samples.

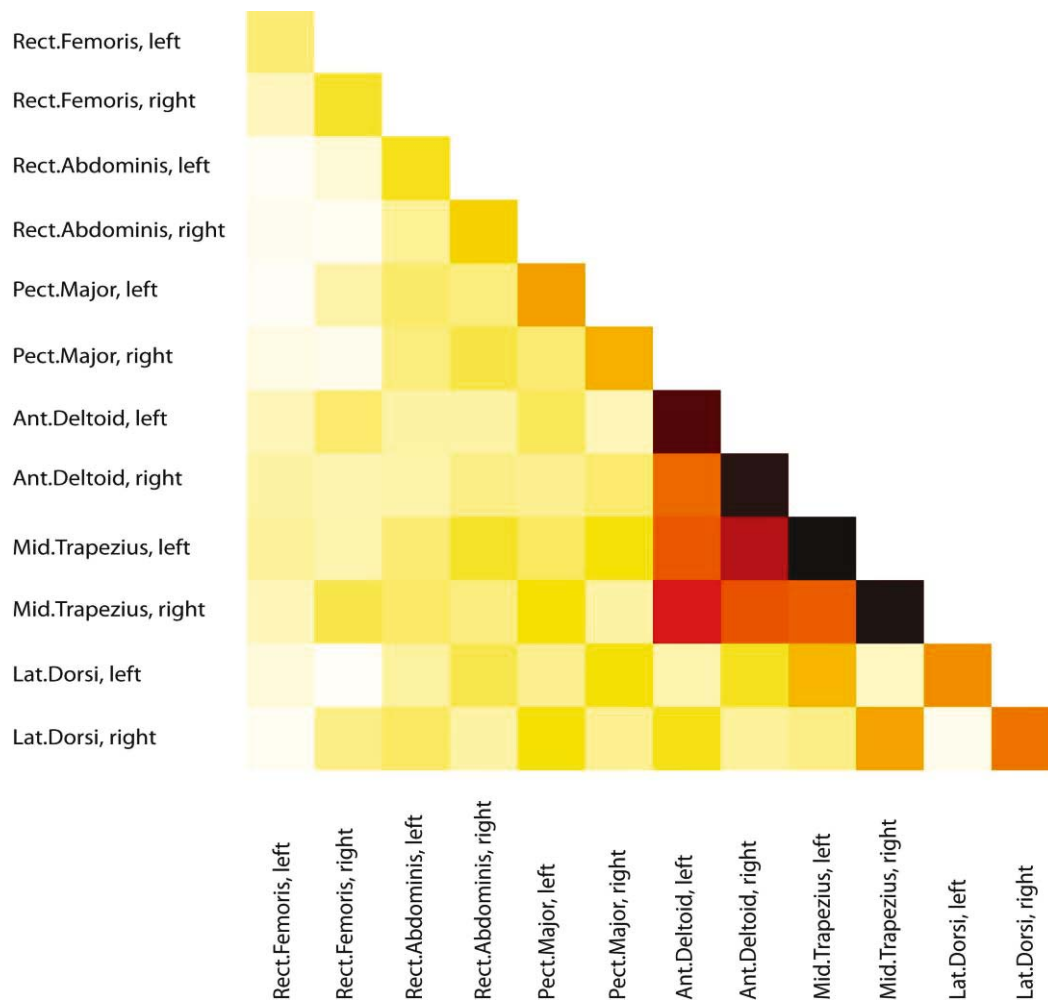


Figure 8. The overall coactivation percentage of different muscles at 70% target output (run 3).

Ant. Deltoid and Middle Trap. muscle groups showed the strongest coactivation. The opposite side muscle combinations have stronger coactivation (left Ant. Deltoid - right Middle Trap.: 38%, right Ant. Deltoid - left Middle Trap.: 42%), while the same-side coactivations have lower values (29% for the right side and 28% for the left side). Lat. Dorsi and Middle Trap. also has a strong coactivation of the same sides: left 20% and right 22%.

Figure 7 shows that by increasing the target normalized output power, more intensity and a broader activity phase are present for almost all muscles. Ant. Deltoid and Middle Trap. exhibit increase in intensity as well, but the range where the muscle is active does not change significantly. The only change is that the start and end points of the period where the muscle is active shifts closer to the start of the tempo.

This information can be used for individual athletes to correct errors and help them to work on the strategy to achieve better muscle coordination similarly as described above for asymmetry and muscle intensity-power analysis.

Muscle intensity correlations

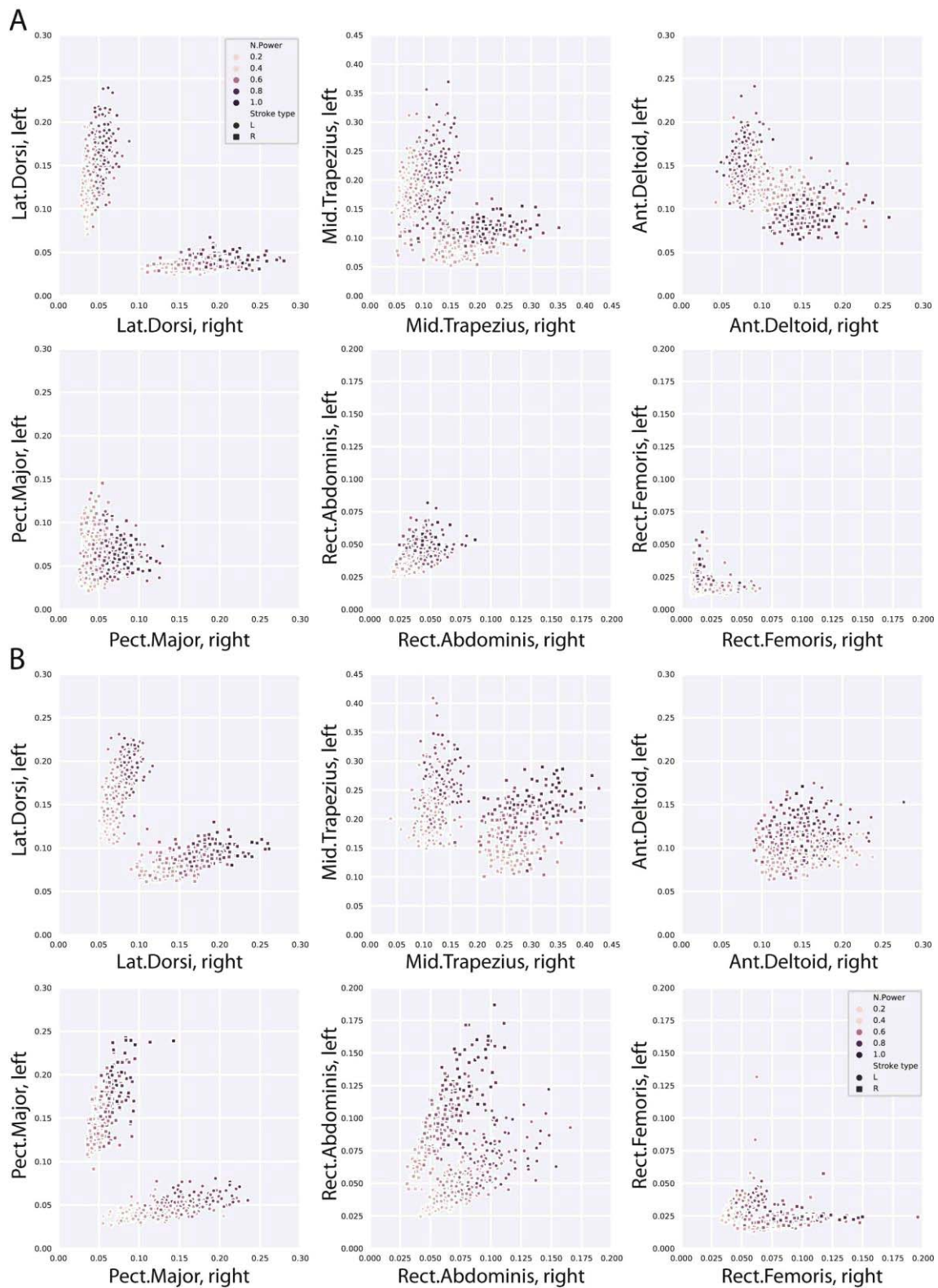


Figure 9. The average intensity of muscle groups during a specific stroke. Squares denote right strokes and circles denote left strokes. The color of the intensity reflects the normalized output power associated with that particular stroke. BP27 (first set of 6 subplots (A), taken from a short distance kayak athlete with a 1st place at a World Championship) and BP39 (second set of 6 subplots (B), a mid-distance kayaker). The unit on the x and y-axis is microvolt.

Figure 9 shows the average intensity of muscle groups from each side during a specific stroke. Squares denote right strokes and circles denote left strokes. The color of the intensity reflects the normalized output power associated with that particular stroke. The plots can be useful to compare the individual characteristics and styles of an athlete to another. For example, BP27 (first set of 6 subplots, representative of a short-distance athlete with a 1st place World Championship) and BP39 (the second set of 6 subplots, originates from a mid-distance kayaker).

We can observe how BP39 uses Ant. Deltoid muscles differently: the left and right stroke are not easily distinguishable from the chart; both of the muscles have similar activities. BP27, however, uses the left Ant. Deltoid more in a left stroke and lets the right Ant. Deltoid rest. One can observe a similar pattern on the right side during the right stroke. Also, BP27 uses Lat. Dorsi muscles differently: having one side of muscles work intensely while the other side entirely rests.

One can see more clustered behavior with Pect. Major and Rectus Abdom. BP27 has these muscle activities more packed, more clustered, however more relaxed overall. It could mean that the BP27 might have more developed muscles and BP27 does not need as much intensity to achieve the same result. Otherwise, this might be a characteristic of how these muscles should behave in order to be extremely efficient.

With these methods, we can perform sophisticated analysis by utilizing the connection between power and muscle coordination/intensities.

Discussion

For both the kayak athlete and coach, receiving objective feedback of the athletes' performance during the training is of pivotal importance. The instructions athletes receive during these sessions will determine how they carry out the training and competition in the desired range of load. The most common feedback, which is, to some degree frequently used, is heart rate monitoring (Borges et al., 2015). One can use the connection between heart rate and metabolism to evaluate individual heart rate zones in which the athlete uses different substrates (e.g., carbohydrates, fatty acids, and others) to provide energy. Training in different zones strengthens the connected processes to provide energy, allowing the athlete to perform better during the related load conditions. While previous groups concluded that there are differences between on-ergometer and on-water kayaking with this regard (Fleming, Donne, & Fletcher, 2012; Fleming, Donne, Fletcher, et al., 2012; Hunter, Cochrane, & Sachlikidis, 2008), ergometer training is still a widely used tool during winter and to study the different aspects of kayaking (Jones & Peeling, 2014; Michael, Rooney, & Smith, 2008; Winchcombe et al., 2019). In our exercise stress – kayak ergometer setting by using the *vita maxima* and *vita sub-maximal* test load profiles, we were able to eliminate anomalies resulting from individual differences in the metabolic background, thus producing physical stress equal for all participants.

A required next step was to be able to increase velocity on the water with the same load or the same effort during kayaking. It is related to the paddling power and technique of the athlete. Several studies observed paddling techniques in controlled environments (in laboratories) using a kayak-ergometer, where they quantified different variables such as electromyogram (EMG) signal of different muscles, stroke force, kinematics (Fleming, Donne, Fletcher, et al., 2012; Michael et al., 2008), different physiological traits, such as heart rate, metabolic values, oxygen consumption (Michael et al., 2008; Tesch, 1983). In our study, we were able to set up personalized targets calculated from the *vita maxima* protocol. We provide immediate feedback to the kayak athletes on how they perform under different target ratios and succeed in reaching and maintaining the power output at a steady level.

Based on our data, if there are more runs with differing goals, a weighting scheme is better to be

applied, with higher weights given to higher goal output and lower weights given to lower goal output powers. While overperforming is generally preferable to underperforming during a training session, it is better to be as close as possible to the goal output power that the coach or trainer gave. Maintaining this constant power is complicated. Significant fluctuations measured in rowing power around a target output mean that the athlete's motion is not fluid; a lower average output period is followed by an increased output period. It is better to have lower variability in the output measurements to maintain the fluidity of motion and stroke length and prevent injuries caused by sudden increases in the movement to get back to the target goal. Measurement of the muscle intensities allows us to study the relationship between output power and the combined intensities of the muscles, understand how they work together, how each of them influences the periodic power outputs, which muscles are active during a stroke. Using this approach, we tested stroke kinematics under maximal exercise load conditions, and we managed to pinpoint specific muscles and activity patterns responsible for the best power output and fluidity of paddling. Earlier seminal EMG studies pinpointed the importance of EMG measurements for stroke kinematics in kayakers (Fleming, Donne, & Mahony, 2014). Our result suggests that kayak athletes should improve the muscle coordination to be similar to the others, which may lead to better results on the ergometer and the field as well (at least for this particular set of muscles or paddling asymmetry). We also described which muscles coactivate during kayaking. This coactivation pattern recognition is individualized, and we intend to correlate these findings with freshwater performance and video analysis.

Conclusions

We developed a continuous performance and biological signal measurement system for recording and processing the performance of athletes on an ergometer under controlled laboratory conditions. We managed to synchronize the commercial sensor signals. We will further analyze the big dataset acquired by artificial intelligence-based algorithms.

Our further plans are developing a closed-loop system that includes an automated analytical software background to provide instant audiovisual feedback towards the athlete and coach and for providing automated performance optimization based on machine and potentially deep learning. We plan to carry out more measurements from athletes and extend the force and EMG measurement with movement analysis. Applying cluster analysis and machine learning for performance development is the next step for our research group.

Acknowledgments

Project no. ED_17-1-2017-0009 has been implemented with the support provided by the National Research, Development and Innovation Fund of Hungary, financed under the National Bionics Program funding scheme. The research project has received support from the Institute of Advanced Studies Kőszeg (iASK).

References

- Bjerkefors, A., Rosén, J. S., Tarassova, O., & Arndt, A. (2019). Three-Dimensional Kinematics and Power Output in Elite Para-Kayakers and Elite Able-Bodied Flat-Water Kayakers. *J Appl Biomech*, 35(2), 93-100. doi:10.1123/jab.2017-0102
- Borges, T. O., Dascombe, B., Bullock, N., & Coutts, A. J. (2015). Physiological characteristics of well-trained junior sprint kayak athletes. *Int J Sports Physiol Perform*, 10(5), 593-599. doi:10.1123/ijsp.2014-0292

- Fleming, N., Donne, B., & Fletcher, D. (2012). Effect of Kayak Ergometer Elastic Tension on Upper Limb EMG Activity and 3D Kinematics. *J Sports Sci Med*, 11(3), 430-437.
- Fleming, N., Donne, B., Fletcher, D., & Mahony, N. (2012). A biomechanical assessment of ergometer task specificity in elite flatwater kayakers. *J Sports Sci Med*, 11(1), 16-25.
- Fleming, N., Donne, B., & Mahony, N. (2014). A comparison of electromyography and stroke kinematics during ergometer and on-water rowing. *J Sports Sci*, 32(12), 1127-1138. doi:10.1080/02640414.2014.886128
- Hunter, A., Cochrane, J., & Sachlikidis, A. (2008). Canoe slalom competition analysis. *Sports Biomech*, 7(1), 24-37. doi:10.1080/14763140701683155
- Jones, M. J., & Peeling, P. (2014). A comparison of laboratory-based kayak testing protocols. *Int J Sports Physiol Perform*, 9(2), 346-351. doi:10.1123/ijsp.2013-0136
- Michael, J. S., Rooney, K. B., & Smith, R. (2008). The metabolic demands of kayaking: a review. *J Sports Sci Med*, 7(1), 1-7.
- R.J.N. Helmer, A. F., J Baker, and I. Blanchonette. *Instrumentation of a kayak paddle to investigate blade/water interactions*. Paper presented at the 5th Asia-Pacific Congress on Sports Technology (APCST).
- Steeves, D., Thornley, L. J., Goreham, J. A., Jordan, M. J., Landry, S. C., & Fowles, J. R. (2019). Reliability and Validity of a Novel Trunk-Strength Assessment for High-Performance Sprint Flat-Water Kayakers. *Int J Sports Physiol Perform*, 14(4), 486-492. doi:10.1123/ijsp.2018-0428
- Tay, C. S., & Kong, P. W. (2018). A Video-Based Method to Quantify Stroke Synchronisation in Crew Boat Sprint Kayaking. *J Hum Kinet*, 65, 45-56. doi:10.2478/hukin-2018-0038
- Tesch, P. A. (1983). Physiological characteristics of elite kayak paddlers. *Can J Appl Sport Sci*, 8(2), 87-91.
- Vadai G., G. Z., Mingesz R. and Mekan G. (2013). *Performance estimation of kayak paddlers based on fluctuation analysis of movement signals*. Paper presented at the IEEE.
- Vadai, G. M., G.; Gingl, Z.; Mingesz, R.; Mellar, J.; Szepe, T.; Csamango, A. (2013). *On-water measurement and analysis system for estimating kayak paddlers' performance*. Paper presented at the Information & Communication Technology Electronics & Microelectronics (MIPRO).
- Winchcombe, C. E., Binnie, M. J., Doyle, M. M., Hogan, C., & Peeling, P. (2019). Development of an On-Water Graded Exercise Test for Flat-Water Sprint Kayak Athletes. *Int J Sports Physiol Perform*, 1244-1249. doi:10.1123/ijsp.2018-0717 www.olympic.org.

Appendix

Arithmetic mean of observations:

$$A = \frac{1}{n} \sum_{i=1}^n a_i = \frac{a_1 + a_2 + \dots + a_n}{n} \quad (1)$$

Correlation between two random variables:

$$r_{xy} = \frac{\sum_{i=1}^n (x_i - \bar{x})(y_i - \bar{y})}{(n-1)s_x s_y} = \frac{\sum_{i=1}^n (x_i - \bar{x})(y_i - \bar{y})}{\sqrt{\sum_{i=1}^n (x_i - \bar{x})^2 \sum_{i=1}^n (y_i - \bar{y})^2}} \quad (2)$$

, where x_i and y_i refers to the samples measured, while s_x , s_y refers to the standard deviations.

Moving average of an observed random variable p :

$$p_{SM}^- = \frac{p_M + p_{M-1} + \dots + p_{M-(n-1)}}{n} = \frac{1}{n} \sum_{i=0}^{n-1} p_{M-i} \quad (3)$$

Root mean squared error of measurements y_i :

$$RMSE = \sqrt{\sum_{i=1}^n \frac{(\hat{y}_i - y_i)^2}{n}} \quad (4)$$

Sample standard deviation:

$$s = \sqrt{\frac{1}{N-1} \sum_{i=1}^N (x_i - \bar{x})^2} \quad (5)$$